Cement & Concrete Composites 34 (2012) 946–957

Contents lists available at SciVerse ScienceDirect

Cement & Concrete Composites

journal homepage: www.elsevier.com/locate/cemconcomp

Structural performance of shear-critical RC deep beams with corroded longitudinal steel reinforcement

Rizwan Azam [a,b], Khaled Soudki [a,*]

[a] Department of Civil Engineering, University of Waterloo, Waterloo, ON, Canada N2L 3G1
[b] Department of Civil Engineering, University of Engineering & Technology, Lahore, Pakistan

ARTICLE INFO

Article history:
Received 1 March 2011
Received in revised form 5 May 2012
Accepted 8 May 2012
Available online 17 May 2012

Keywords:
Corrosion
Shear
Reinforced concrete
Deep beams
FRP repair

ABSTRACT

The effect of corrosion of longitudinal reinforcement on the structural performance of shear-critical reinforced concrete (RC) deep beams was experimentally investigated. A total of eight medium-scale reinforced concrete beams were constructed. The beams measured 150 mm wide, 350 mm deep and 1400 mm in length. The test variables included: corrosion levels (0%, 5%, and 7.5%), existence of stirrups and FRP repair. Six beams were subjected to artificial corrosion whereas two beams acted as control un-corroded. Following the corrosion phase, all beams were tested to failure in three point bending. The test results revealed that corrosion of properly anchored longitudinal steel reinforcement does not have any adverse effect on the behaviour of shear critical RC deep beams. Corrosion changed the load transfer mechanism to a pure arch action and as a result the load carrying capacity was improved. A strut and tie model was proposed to predict the failure loads of shear-critical RC deep beams with corroded longitudinal steel reinforcement. The predicted results correlated well with the experimental results.

1. Introduction

Shear of reinforced concrete (RC) beams is a complex phenomenon that is still not very well understood. In general, shear mechanism and failure mode of reinforced concrete beams depends on the shear span to depth ratio (a/d). Beams with a/d ratio greater than 2.5 are considered slender beams and fail by diagonal tension failure (an inclined tensile crack penetrates through the compression zone) whereas beams with a/d ratio less than 2.5 are deep beams and fail by shear compression failure (concrete crushing occurs at the tip of the shear crack in compression zone). Because of their different failure mechanisms, deep and slender beams are studied separately [1–3].

Corrosion of reinforcing steel is the most significant deterioration problem faced by reinforced concrete structures. The exposure of reinforced concrete structures to deicing salts and marine environment causes corrosion of the embedded reinforcing steel. Corrosion products occupy more volume than the original reinforcing steel thus resulting in cracking and spalling of the surrounding concrete. Corrosion of the steel reinforcement results in loss of bond between reinforcing steel and concrete and a reduction in cross-sectional area of the reinforcing bar.

A number of studies have been reported in the literature to investigate the effect of corrosion of the reinforcing steel on reinforced concrete members. The majority of the previous studies have focused on flexural and bond strength of corroded beams [4–9]. There are only few studies related to the shear strength of corroded beams; specially, shear strength of corroded deep beams [10–12]. These studies [10–12] have incorporated corrosion either on the stirrups only [10,11] or on both the stirrups and longitudinal reinforcement [12] to investigate the effect of corrosion on the shear strength of RC beams. The effect of corrosion of the stirrups on shear strength of deep beams revealed that there is a significant reduction in strength in beams with corroded stirrups and that a beam with significant stirrups corrosion may fail by diagonal tension failure instead of shear compression failure [10,11].

To the author's knowledge, there is no information in the literature on the effect of corrosion of longitudinal reinforcement on the shear strength of reinforced concrete deep beams. This study was designed to investigate the effect of corrosion of the longitudinal reinforcement on the behaviour of shear-critical reinforced concrete deep beams constructed without shear reinforcement and with minimum shear reinforcement and to examine FRP repair for such beams.

2. Experimental program

A total of eight shear critical reinforced concrete deep beams were constructed and tested. The beams were divided into two series: series A – beams without stirrups and series B – beams with stirrups. Each series contained four beams: one control un-corroded beam, two corroded beams and one corroded FRP repaired beam.

* Corresponding author.
E-mail addresses: razam@engmail.uwaterloo.ca (R. Azam), Soudki@uwaterloo.ca (K. Soudki).

0958-9465/$ - see front matter © 2012 Elsevier Ltd. All rights reserved.
http://dx.doi.org/10.1016/j.cemconcomp.2012.05.003

The test variables included the corrosion level (none, medium and high), presence or absence of stirrups and FRP repair. Table 1 summarises the test matrix.

2.1. Test specimens

The details of the test specimens are presented in Fig. 1. All beams were 150 mm × 350 mm in cross section and 1400 mm long. The longitudinal tensile reinforcements were 2-25M bottom bars with standard 90° hooks. The side and vertical covers to the tension reinforcement were 30 mm. The compression reinforcements were 2-10M bars. The stirrups used were 6 mm smooth bars at 215 mm spacing with three additional stirrups provided in the anchorage zone. Stirrup spacing was according to CSA A23.3-94. A corroded beam had corroded and un-corroded zones with shaded area representing the salted concrete as shown in Fig. 1. The longitudinal tensile reinforcements were corroded in the corroded zone and the stirrups were epoxy coated to prevent them from corrosion. A stainless steel hollow tube with a diameter of 15 mm and wall thickness of 0.89 mm placed at 125 mm from the bottom of beams was used as a cathode in accelerated corrosion process.

Salted and unsalted concrete was used to construct the test beams. The concrete was batched with Type-10 Portland cement with a maximum coarse aggregate size of 19 mm and a water/cement ratio of 0.55. The salted concrete contained 2.3% chlorides by mass of cement. The average compressive strength of the salted and unsalted concrete at the time of beam testing was 51.7 ± 5.12 MPa and 47.3 ± 0.68 MPa, respectively. The longitudinal reinforcements were grade 400 reinforcing steel bars and stirrups had nominal yield strength of 384 MPa.

2.2. Accelerated corrosion

Six beams were subjected to accelerated corrosion by impressing a direct current into the longitudinal bars at a constant current density of 150 μA/cm^2 using power supplies [13]. The longitudinal reinforcing bars acted as the anode and the stainless steel tube acted as a cathode in this artificial corrosion cell. To disrupt the passive layer around the reinforcing bar embedded in the concrete, salt was mixed in the concrete during casting of the beams. The beams were corroded in series in groups of three beams. A schematic diagram showing the details of the connection between the longitudinal reinforcing bars, the stainless steel tube and the power supply is shown in Fig. 2.

The beams were placed inside a corrosion chamber that maintained the humid environment (moisture and oxygen) by a mist nozzle. The time required to corrode the reinforcing steel bars to 5% and 7.5% mass loss was calculated based on Faraday's law as 66 days and 99 days.

2.3. Instrumentation

Electrical resistance strain gauges were attached on the two longitudinal bars (gauge length of 5 mm) and on the concrete (60 mm gauge length) in the control specimens. No gauges were installed on the reinforcement in the corroded beams since they would be destroyed during the accelerated corrosion. The layout of the strain gauges, used to monitor the behaviour of beams, is shown in Fig. 3.

Two linear variable differential transducers (LVDTs) one at each side of the beam, with a range of 25 mm, were placed at mid-span to measure the deflection of the beam as shown in Fig. 5.

2.4. FRP repair

Two corroded beams (7.5% corrosion level) were repaired with carbon fibre reinforced polymer (CFRP) sheets. Intermittent CFRP U-wraps were used as shown schematically in Fig. 4. The CFRP sheets were Sika Wrap 230C and the epoxy resin was Sikadur 330. The application of the CFRP repair followed the manufacturer's specifications. The concrete surfaces were sand blasted and cleaned to get rid of the corrosion staining on the beam surface and to expose the aggregates. The edges of the beam cross section were rounded. Sikadur 330 epoxy resin was applied on the concrete surface. Then the CFRP sheet was placed by hand. A steel roller was used to apply pressure on the CFRP sheet to remove air pockets. The beams were left for 7 days to allow curing of the CFRP system.

2.5. Test setup and procedure

The beams were tested in three-point bending using a closed-loop hydraulic MTS actuator with a 500 kN capacity in a Uniroyal test frame as shown in Fig. 5. The beams were simply supported over a clear span of 1000 mm and loaded with one concentrated point at mid-span. The loading plate was potted to the beam using hydro-stone. The load was increased monotonically in displacement control with a rate of 0.05 mm/min until failure of beam. The readings of the instrumentation (LVDT's and strain gauges) were recorded using a data acquisition system. During the test, the initiation and progression of cracks was monitored.

3. Test results and discussion

3.1. Corrosion cracking and mass loss

Corrosion cracking in terms of crack patterns and crack widths were recorded using a crack comparator (with a resolution of 0.15 mm) for all corroded beams at the final stages of corrosion.

Table 1
Details of test specimens.

Specimen		Target $f'c$ (MPa)	Longitudinal reinforcement				Shear reinforcement
			Amount of reinforcement	ρ (%)	$\rho/\rho b$	Corrosion level	
Series-A (beams without stirrup)	L-0%	40	2-25M bars	2.17	0.50	None	–
	L-5%	40	2-25M bars	2.17	0.50	Medium	–
	L-7.5%	40	2-25M bars	2.17	0.50	High	–
	L-7.5%-R	40	2-25M bars	2.17	0.50	High	–
Series-B (beams with stirrup)	LS-0%	40	2-25M bars	2.17	0.50	None	6 mm@215 mm c/c
	LS-5%	40	2-25M bars	2.17	0.50	Medium	6 mm@215 mm c/c
	LS-7.5%	40	2-25M bars	2.17	0.50	High	6 mm@215 mm c/c
	LS-75%-R	40	2-25M bars	2.17	0.50	High	6 mm@215 mm c/c

Beam reinforcement specified as L (only longitudinal reinforcement) and LS (longitudinal and transverse reinforcement).
Corrosion level specified as 0% (none), 5% (medium), and 7.5% (high).
FRP reinforcement specified with letter "R".

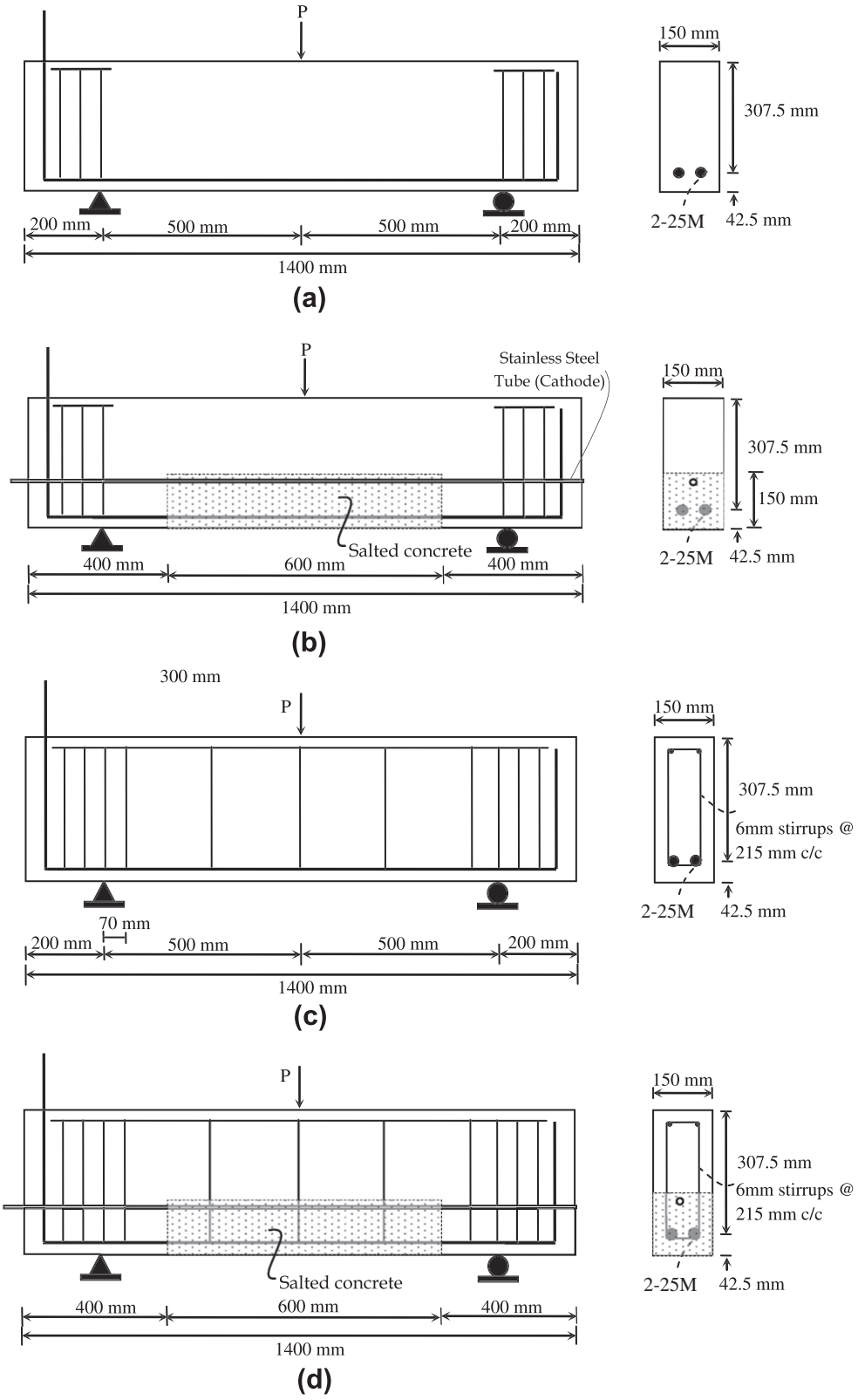

Fig. 1. Details of specimens (a) control beam without stirrups, (b) corroded beam without stirrups, (c) control beam with stirrups and (d) corroded beam with stirrups.

Different types of corrosion crack patterns were observed (Fig. 6): some beams had two longitudinal cracks, both at the bottom soffit of the beam running parallel to the longitudinal reinforcement; some beams had one crack at the bottom soffit and another crack on the side of the beam; some beams had cracks on the two sides of the beam; some beams had irregular cracks (cracks starting from the bottom soffit of the beam that moved to the side of the beam). The possible reasons for these observed crack patterns could be that the corrosion products may not have been uniformly distributed around the cross section of the bar

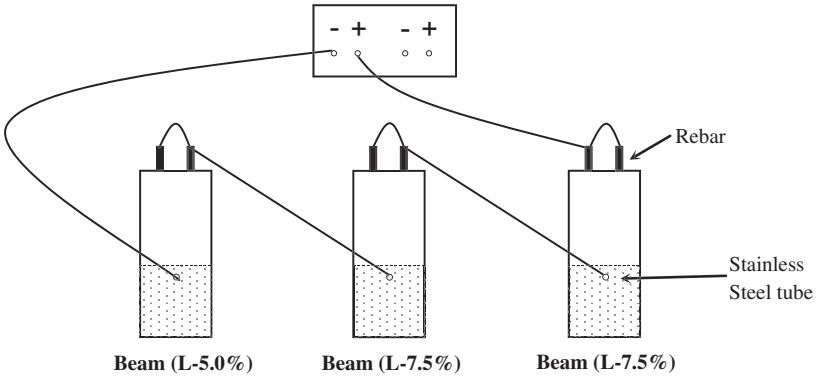

Fig. 2. Schematic diagram of accelerated corrosion circuit.

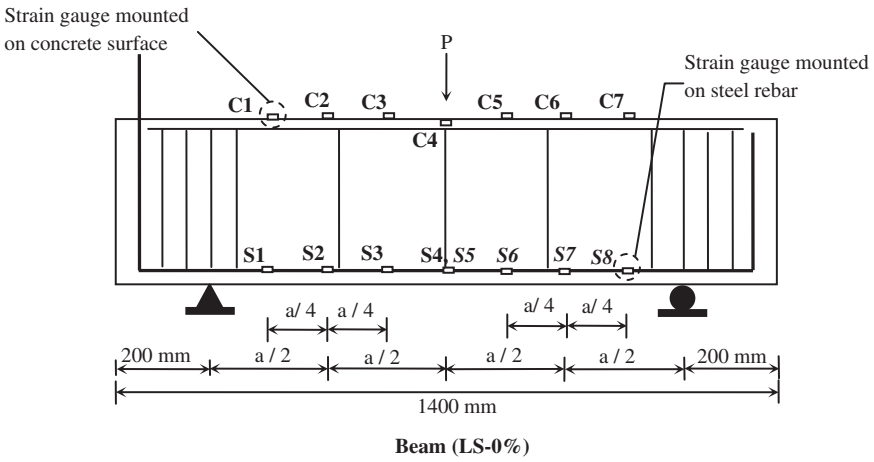

Fig. 3. Locations of strain gauges along the beam.

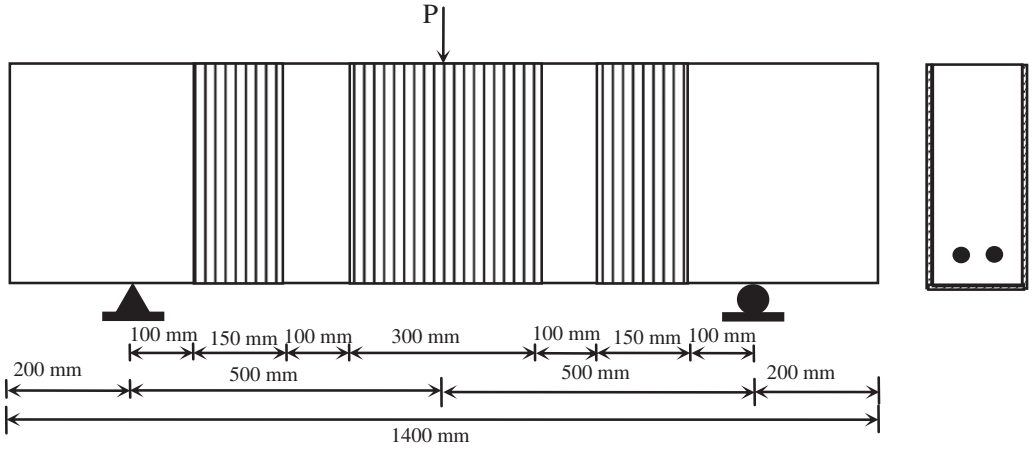

Fig. 4. FRP repair scheme.

and that the concrete cover may have shifted during placement of cage.

The maximum crack widths in deep beams without stirrups were 1.25 mm and 1.5 mm at 5% and 7.5% theoretical corrosion level, respectively. The maximum crack widths in the deep beams with stirrups were 1.0 mm and 1.5 mm at 5% and 7.5% theoretical corrosion level, respectively.

The actual mass loss due to steel reinforcement corrosion was measured using carefully extracted bars from the corroded beams following the load testing phase. The procedure given in ASTM standard GI, designation C.3.5 was used for the mass loss analysis [14]. Four coupons, two from each bar, 300 mm in length were taken from each corroded beam. Coupons from the control beams were used as a reference. Table 2 summarises the mass loss results.

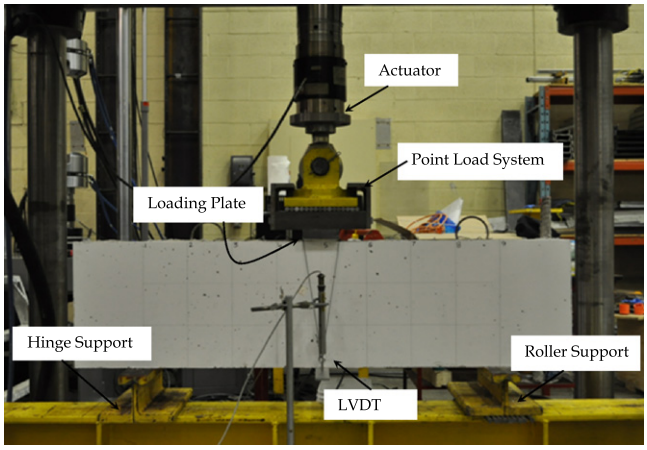

Fig. 5. Test setup.

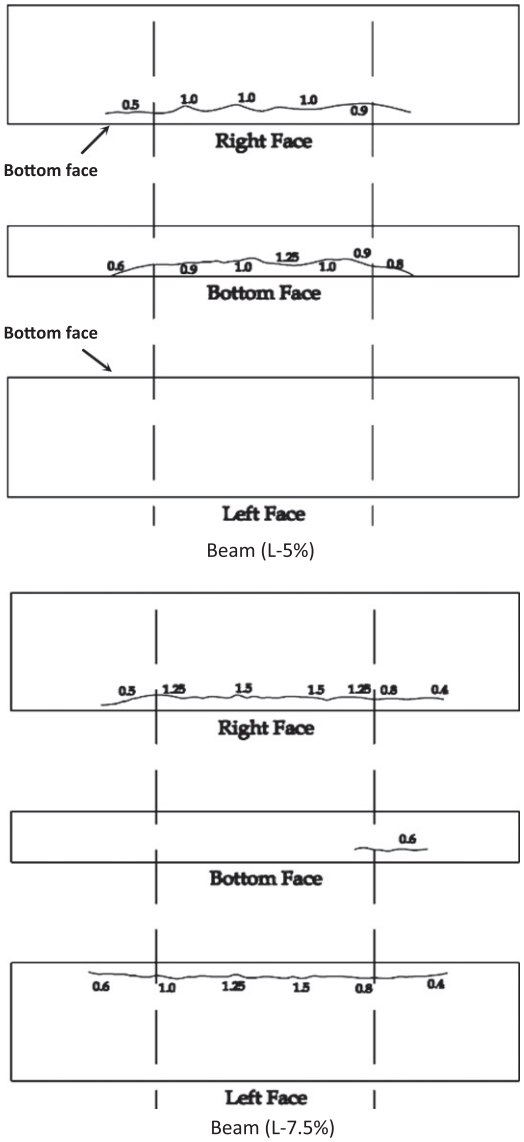

Fig. 6. Typical corrosion crack patterns and crack widths (all crack widths are in mm).

Table 2
Theoretical and experimental mass loss.

Beam designation	Theoretical mass loss (%)	Experimental mass loss (%)
L-5.0%	5.0	4.38 ± 0.40
L-7.5%	7.5	4.64 ± 0.20
L-7.5%-R	7.5	2.45 ± 0.23
LS-5.0%	5.0	3.85 ± 0.45
LS-7.5%	7.5	4.49 ± 0.42
LS-7.5%-R	7.5	4.47 ± 0.39

The average measured mass loss for all beams was 4.1% and 4.5% for 5.0% and 7.5% theoretical mass loss. The target mass loss was not achieved at higher corrosion a level which is consistent with findings of other researchers [15,16].

3.2. Structural behaviour

A summary of the test results is presented in Table 3. The structural behaviour will be discussed in terms of strain response, failure modes and load deflection response.

3.2.1. Strain response

The measured strain profiles in the longitudinal steel reinforcement and the concrete surface of the control beams (Figs. 7 and 8) illustrate the load transfer mechanism in deep beams. Before inclined cracking, the beam behaved according to beam theory. The strain values in the longitudinal bar and on the concrete surface varied linearly up to inclined cracking (the inclined cracking loads for Series A and B beams were 151 kN (0.78P) and 146 kN (0.35P), respectively) as shown in Figs. 7 and 8. After inclined cracking, the beam started to behave as tied arch. The strains in the longitudinal bar were almost constant over the entire clear span of the beam and slightly higher near the supports. At higher load levels, the longitudinal steel tried to straighten the 90° hook on the end of the longitudinal bar in the anchorage zone, which caused tension in the concrete at the top surface of the beam near the support as shown in Figs. 7b and 8b. The contribution of arch action in Series B (beams with stirrups) was 65% of the total loads as compared to Series A (beams without stirrups) which was only 22% of the total load. At failure, the strain values in the steel were below the yield strain and the strains in concrete were also below crushing strain.

3.2.2. Failure modes

The failure modes for the beams without and with stirrups (Series A and B) are shown in Figs. 9 and 10, respectively. The cracking patterns and failure modes of the control (un-corroded) and corroded beams were different. The control beams failed in shear compression failure while the corroded beams failed by splitting of the strut. In the control beams, cracking was initiated with the appearance of flexural cracks under the concentrated load. As the load was increased, inclined cracks appeared in the shear spans. At this stage, the beam continued to carry load until concrete crushing at the tip of the inclined crack that caused shear-compression failure. The cracking in the corroded beams was also initiated with the appearance of flexural cracks under the concentrated load but these cracks progressed towards the compression zone as the load increased. The beams kept carrying load until sudden failure by splitting of struts. The corroded beams did not experience any inclined/shear cracking except for a single diagonal crack which appeared at failure due to splitting of the strut.

3.2.3. Load deflection response

In general, the load deflection response for all the beams was bilinear, indicating the brittle nature of shear failure. The stiffness

Table 3
Summary of test results.

Beams		Tested $f'c$ (MPa)	Measured mass loss (%)	Inclined cracking load (kN)	Ultimate load (kN)	Deflection at ultimate load (mm)	Failure mode
Beams without stirrups (Series-A)	L-0%	47.3	–	151	191.63	2.0	Shear-compression
	L-5%	47.3	4.38	–	476.4	3.90	Splitting of strut
	L-7.5%	47.3	4.64	–	476.17	3.88	Splitting of strut
	L-7.5%-R	47.3	2.45	–	497.13	3.37	Splitting of strut
Beams with stirrups (Series-B)	LS-0%	47.3	–	146	418.41	3.85	Shear-compression
	LS-5%	47.3	3.85	–	386.17	2.74	Splitting of strut
	LS-7.5%	47.3	4.49	–	422.85	3.22	Splitting of strut
	LS-7.5%-R	47.3	4.47	–	447.44	3.54	Splitting of strut

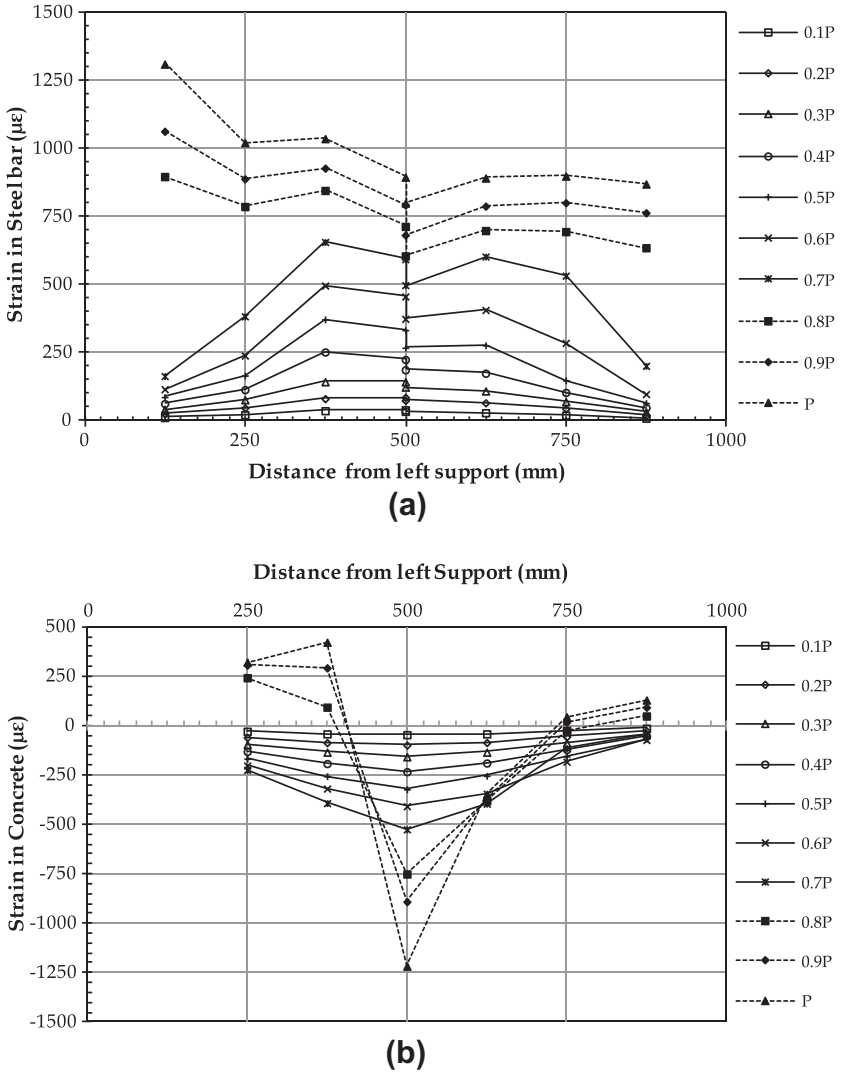

Fig. 7. Strain profiles in Series-A control beam (a) in longitudinal bars (b) at top surface of concrete.

reduction occurred at the onset of inclined/shear cracking in the control beams while the stiffness reduction occurred at onset of flexural cracking in corroded beams.

3.2.3.1. Effect of corrosion. The influence of corrosion on the structural behaviour of beams with properly anchored longitudinal reinforcement is presented first. Fig. 11a shows the effect of corrosion of properly anchored longitudinal reinforcement on the load deflection behaviour of beams without stirrups (Series A). The control un-corroded beam failed in shear compression failure at a load of 192 kN. The beams that were corroded to 4.4% and 4.6% mass loss had a different mode of failure (splitting of the compression strut) and failed at the same failure load of 476 kN (Table 3). Corrosion led to a change in the load transfer mechanism from a combination of beam and arch action in the control beam to a pure arch action in corroded beams and resulted in significant increase in the ultimate load of corroded beams. The average increase in the ultimate load of the corroded beams was 150% compared to the

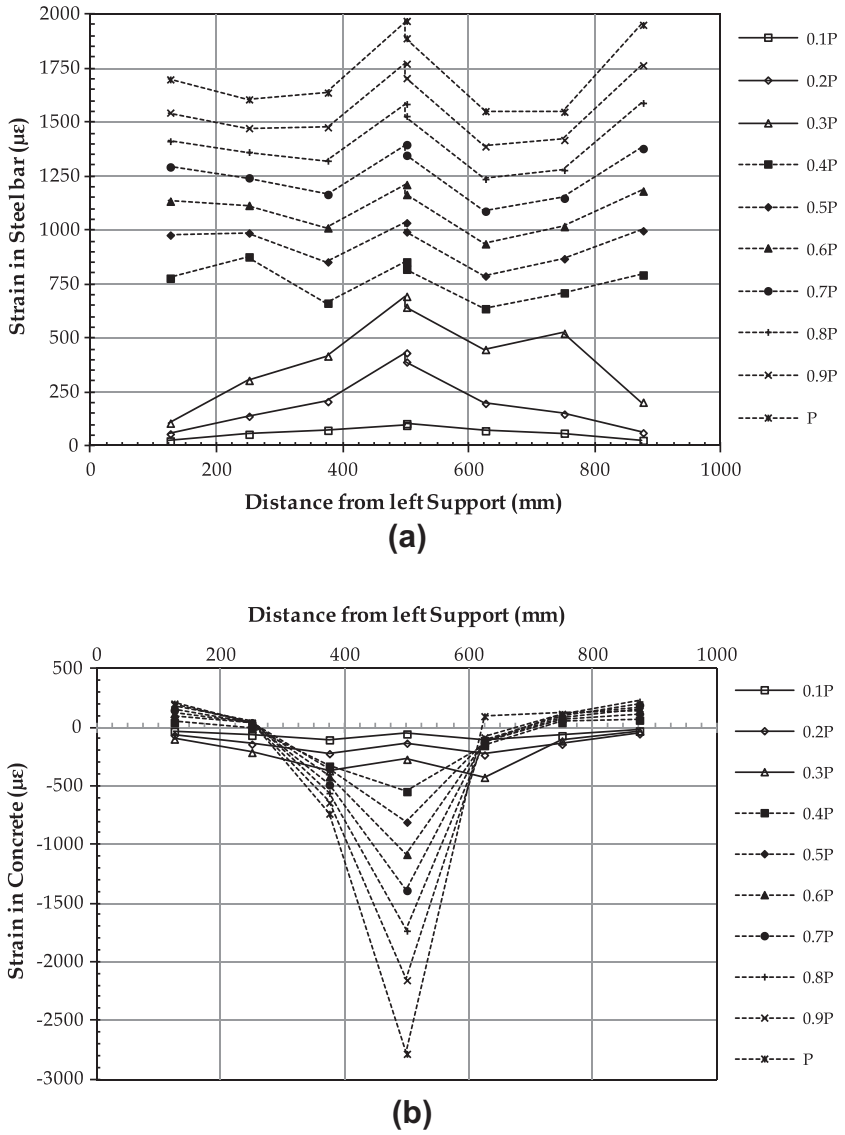

Fig. 8. Strain profiles in Series-B control beam (a) in longitudinal bars (b) at top surface of concrete.

control un-corroded beam. The increase in deflection at the ultimate load in the corroded beams was on average 100% from 2.0 mm in the un-corroded beam to an average of 3.9 mm for the corroded beams.

Fig. 11b shows the effect of corrosion of properly anchored longitudinal reinforcement on load deflection behaviour of beams with stirrups (Series B). The control un-corroded beam failed in shear compression at a load of 418 kN. The beams that were corroded to a mass loss of 3.9% and 4.5% failed by splitting of compression strut at loads of 386 kN and 423 kN, respectively (Table 3). The corroded beams failed at similar load levels to that of the control un-corroded beam. The slight variation in the ultimate strength may be attributed to the variation in concrete strength. The deflection at the ultimate load in the corroded beams was lower compared to the control un-corroded beam. The higher deflection in the control beam is mainly attributed to the shear deformation due to the inclined shear cracking.

Corrosion of longitudinal reinforcement caused a change of load transfer mechanism from a combination of beam and arch action in the control beams to a pure arch action in the corroded beams. The debonding of the longitudinal reinforcement due to corrosion cracking forced the corroded beams to transfer the load in arch action from zero load until failure. Corrosion of the longitudinal reinforcement also altered the shear cracking behaviour of the beams; the control un-corroded beams experienced inclined cracking, while the corroded beams did not have inclined cracking. This resulted in the load being transferred directly from the load point to the support through arch action.

3.2.3.2. Effect of stirrups. The effect of stirrups on the load deflection behaviour of the control and corroded deep beams is presented in Fig. 12a and b. It is evident that the presence of shear stirrups changed the beam failure mode and significantly increased the ultimate load of the control un-corroded beams. The control beam without stirrups failed at a load of 191 kN while the control beam with stirrups failed at a load of 418 kN, which is more than double that of the control (Table 3).

In the control beam without stirrups, once the inclined crack appeared, it quickly progressed towards the compression zone, leaving a small nodal zone area in the cross section to carry the

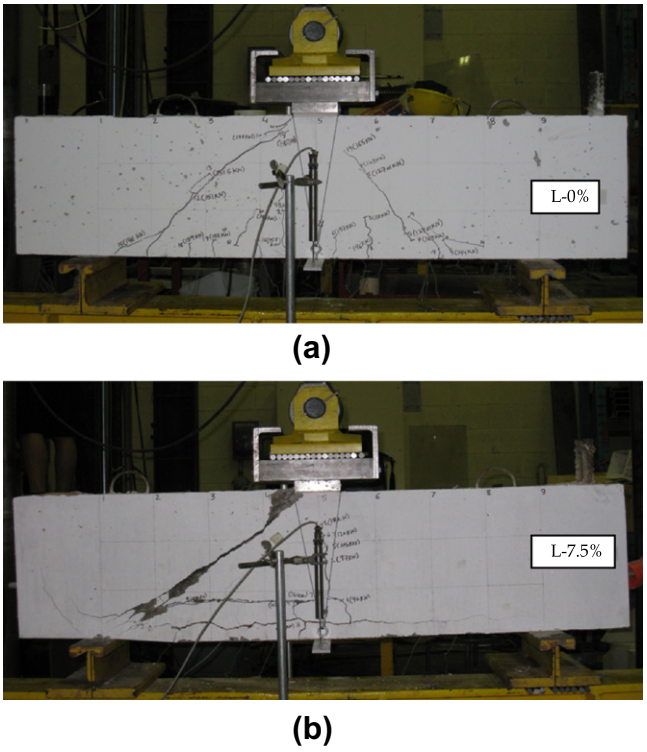

Fig. 9. Series A (a) failure mode of control beam and (b) typical failure mode of corroded beam.

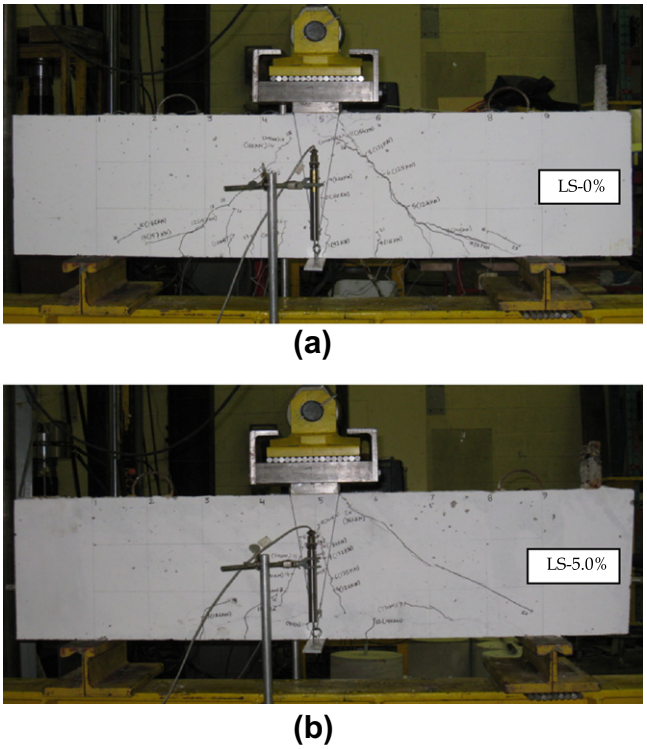

Fig. 10. Series B (a) failure mode of control beam and (b) typical failure mode of corroded beam.

compressive forces in the strut. This caused the beam to fail by concrete crushing under the concentrated load. Conversely, in the control beam with stirrups the propagation of inclined cracks was arrested by the stirrups leaving a relatively greater nodal zone area in the beam. As a result, crushing of the nodal zone was delayed and the beam with stirrups sustained a higher failure load through arch action as compared to the beam without stirrups. The compression reinforcement in beams with stirrups also helped in delaying the crushing of the nodal zone.

The corroded beams without stirrups (L-5% and L-7.5%) failed at a load of 476.4 kN and 476.2 kN while the corroded beam with stirrups (LS-5% and LS-7.5%) failed at a load of 386 kN and 422 kN. Corroded beams with stirrups had on average a 15% reduction in the capacity relative to beams without stirrups (Table 3). It should be noted that the beam with stirrups contained 2-10M bars as compression reinforcement while the beam without stirrups had no compression reinforcement. A beam with compression reinforcement has a smaller strut compared to a beam without compression steel. This will lead to an earlier failure of the strut in the beam with stirrups (with compression steel) than a beam without stirrups (without compression reinforcement). Hence, the beam with stirrups (which contained compression reinforcement) is expected to fail at a lower load in comparison to the beam without stirrups (no compression steel) as observed in the experimental results.

3.2.3.3. Effect of FRP repair. Fig. 13a and b illustrate the effect of FRP repair on the behaviour of corroded beams without stirrups (Series A) and with stirrups (Series B). The load deflection response of the corroded and FRP repaired beams was similar to that of the corroded beam. The failure modes of the FRP repaired corroded beam was also similar to that of the corroded beam. However, FRP confinement delayed the failure crack until the FRP sheets debonded from the concrete surface. The FRP repair of a corroded beam slightly increased its ultimate strength and stiffness in comparison to the corroded beam. The strength of FRP repaired corroded beam was on average 5% higher than that of the corroded beam (Table 3). The increase in stiffness was about 15% for the FRP repaired beams vs. the unrepaired beams (Table 3). The slight increase in load is due to premature debonding of the FRP U wrap. One would expect that if the beams were fully wrapped, higher load would be achieved. The FRP U-wrap delayed the occurrence of the initial flexural cracking which led to attaining a higher load in the FRP repaired beam. The increase in stiffness is possibly due to the increased bond strength between the corroded steel and concrete resulting from FRP confinement.

4. Analytical model

The strut and tie model given in CSA A23.3-04 for shear strength prediction of deep beams does not include the effect of corrosion [17]. In this study, the corroded deep beams failed differently than the control (un-corroded) deep beams. The control deep beams experienced shear cracking while the corroded beams did not. Therefore, a simplified strut-and-tie model is proposed to predict the strength for the corroded deep beams. The model is shown in Fig. 14 and the analysis is described below.

4.1. Analysis procedure

The first step is to establish the geometry of the strut and tie model. The width of the strut is based on the width of the bearing plate (loading plate and reaction plate), the neutral axis depth (c) and the height of the centroid of the tension reinforcement (d'). The upper end of the strut starts from one end of the loading plate and ends at double the height of the centroid of the tension reinforcement above the reaction plate ($2d'$). The lower end of the strut starts from the neutral axis under the loading plate and ends at the other end of the reaction plate. The neutral axis is determined using flexural analysis of the reinforced concrete beam considering the tension and compression reinforcement.

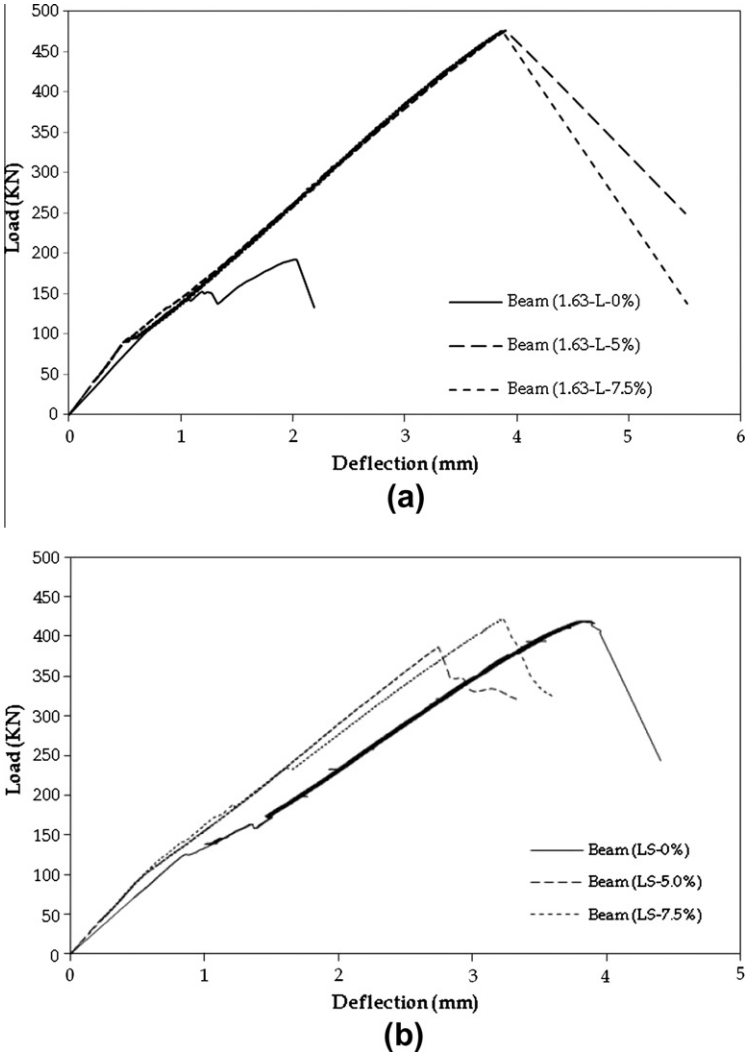

Fig. 11. Effect of corrosion on deep beams (a) Series A-w/o stirrups and (b) Series B-with stirrups.

The second step is to calculate the beam capacity.

The capacity of the corroded deep beams can be determined as the smaller value of the following (Fig. 14):

- Load causing failure due to splitting of the strut (check-1).
- Load causing failure due to yielding of the longitudinal steel reinforcement (check-2).

4.2. Check 1 – failure due to splitting of the strut

In a strut and tie model, the struts are subjected to compressive stresses. The compression in the diagonal struts spread out to maintain the compatibility of the concrete causing transverse tension near the mid height of the strut. If appropriate reinforcement is not provided, the beam will fail by splitting of the strut. Adebar and Zhou [18] recommended a stress limit of $0.6f'c$ for beams with no bearing confinement to the struts, in order to avoid the failure in deep beams by splitting of the strut. In this study, a compressive stress limit of $0.6f'c$ is used. The failure load due to splitting of the strut can be determined using the following equations:

$$P = 2 \cdot V \tag{1}$$

$$V = C \cdot \sin\theta \tag{2}$$

$$C = (0.6f'c) \cdot w_c \times b \tag{3}$$

where P is the failure load; V is the reaction at the support (shear force); C is the compression force in the strut; θ is the angle between strut and tie; $0.6f'c$ is the limiting stress in the strut; $(w_c \times b)$ is the area of the strut; $f'c$ is the compressive strength of concrete; w_c is width of the strut and b is the width of the beam.

4.3. Check 2 – failure due to yielding of longitudinal steel reinforcement

In a strut and tie model, the tie (tension reinforcement) is subjected to a tensile force. Corrosion of tension reinforcement may lead to yielding of tension reinforcement at lower loads. When the beam capacity is governed by the yield strength of the reinforcement, the tension force in the tie is determined by multiplying the yield stress in the reinforcing steel by the cross sectional area of reinforcing bar. Then the capacity of the beam is calculated based on equilibrium of the strut and tie as shown in Fig. 14. The effect of corrosion is considered by reducing the area of the reinforcing bar depending on the actual mass loss. The failure load due to yielding of longitudinal reinforcement can be determined using Eq. (1) and Eqs. (4)–(6).

$$V = T \cdot \tan\theta \tag{4}$$

$$T = \mathrm{As}^* \times F_y \tag{5}$$

$$\mathrm{As}^* = \mathrm{As}(1 - \text{mass loss}\%) \tag{6}$$

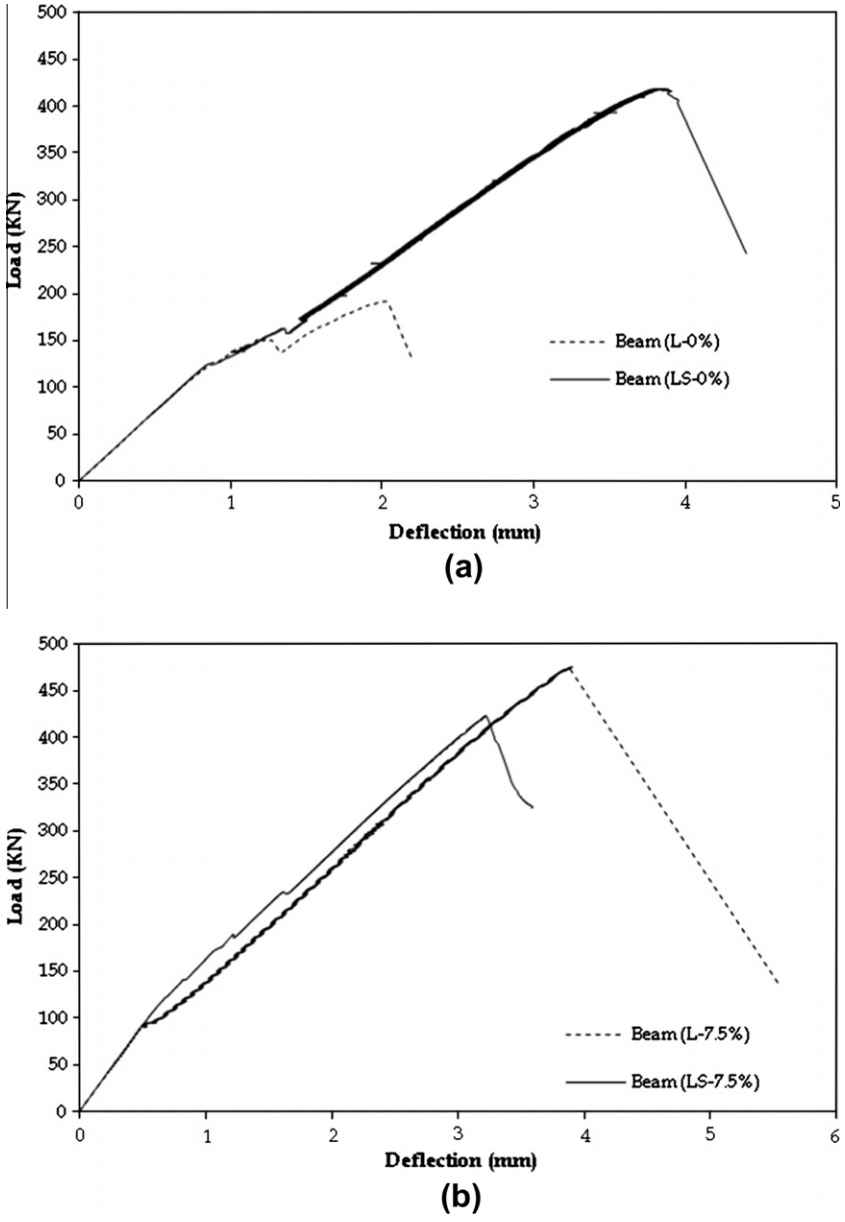

Fig. 12. Effect of stirrups on deep beams (a) control and (b) corroded.

Table 4
Experimental and predicted ultimate loads for the corroded beams.

Beam		Experimental ultimate load (kN)	Predicted ultimate load (kN)	Experimental/ predicted
Series A	L-5.0%	476.4	404.5	1.18
	L-7.5%	476.17	404.5	1.18
Series B	LS-5.0%	386.17	361.1	1.07
	LS-7.5%	422.85	361.1	1.17

where T is the tension force in the tie; θ is the angle between strut and tie; As and As* are the original and corrosion-reduced cross sectional areas of a steel bar and F_y is the yield strength of the steel rebar.

4.4. Predicted results

The ultimate strengths of the corroded beams were predicted using the proposed strut and tie model. The predicted and experimental ultimate loads of the corroded beams are given in Table 4. It is evident from that the predicted failure loads correlated very well with the experimental failure loads with an average ratio of 1.15.

Using the proposed model, the effect of different corrosion levels and concrete strengths on the behaviour of such beams was examined. The failure mode of the beams would change from splitting of struts to yielding of longitudinal reinforcement at higher concrete strength and higher corrosion levels. For example, for current beams ($f'c = 47.3$) the failure mode would change from splitting of strut to yielding of the longitudinal reinforcement at corrosion level of 10%. However, at lower concrete strengths ($f'c < 47.3$ MPa) and lower corrosion levels (<10%) such beams would always fail by splitting of the struts.

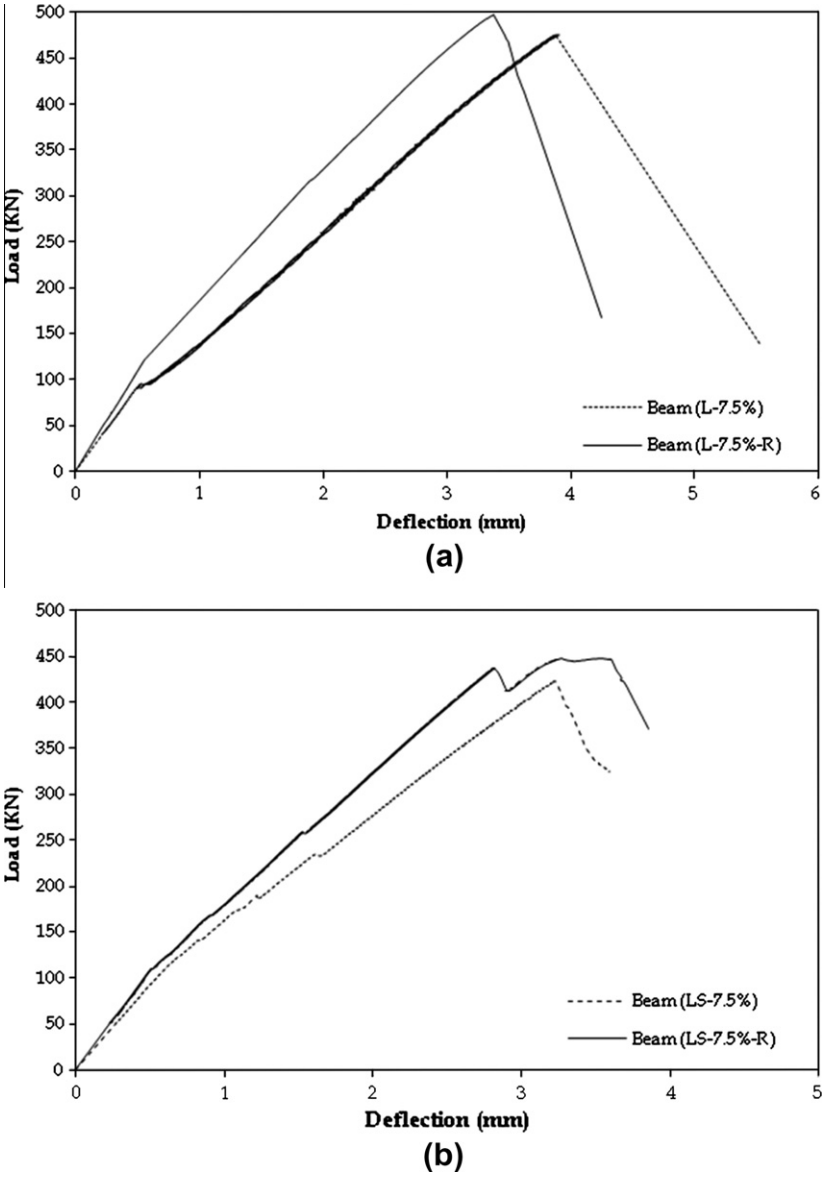

Fig. 13. Effect of FRP repair on corroded deep beams (a) Series A-w/o stirrups and (b) Series B-w stirrups.

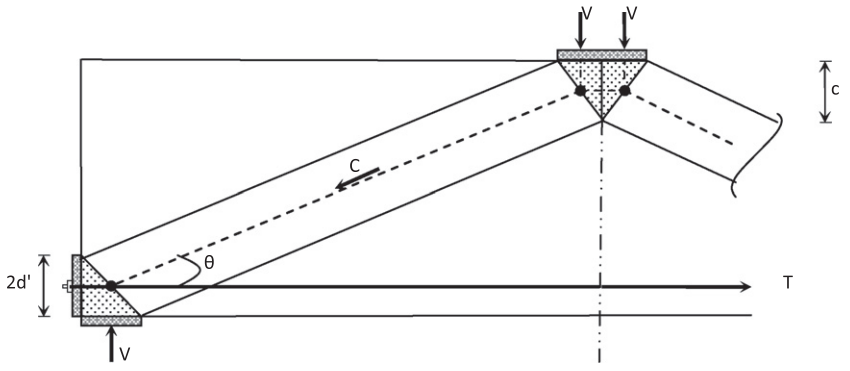

Fig. 14. Proposed strut and tie model for deep beams.

5. Conclusions

The effect of corrosion of the longitudinal reinforcement on the behaviour of shear-critical reinforced concrete (RC) deep beams was investigated. Corrosion induced cracking affected the behaviour of shear critical RC deep beams in two ways. Firstly, it caused debonding of the longitudinal reinforcement that forced the corroded beams to transfer the load in the form of a tied arch compared to combination of beam and arch action in the control un-corroded beams. Secondly, it altered the cracking pattern of

the corroded beam under load. The corroded beam did not experience any shear cracking and the load was transferred directly from the load point to the support through concrete struts. This resulted in failure of the corroded beams by splitting of the concrete strut compared to concrete crushing at the end of the shear crack (shear compression failure) in the control un-corroded beams. The change in load transfer mechanism resulted in an increase in the ultimate load of the corroded beams without stirrups but did not significantly affect the ultimate load of the corroded beams with stirrups. A Strut and tie model was proposed to predict the capacity of corroded shear critical reinforced concrete deep beams. The specific conclusions are as follows:

- Corrosion of the longitudinal reinforcement changed the load transfer mechanism in shear-critical reinforced concrete deep beams; the corroded deep beams transferred the load by pure arch action compared to a combination of beam and arch action in the control un-corroded deep beams.
- The failure mode of the corroded beams was different from control beams. The corroded deep beams failed by splitting of the compression strut compared to shear compression failure in the control un-corroded beams.
- The ultimate strength of corroded deep beams without stirrups was on average 150% higher than the control beams. Corrosion had no significant effect on ultimate strength of deep beams with stirrups.
- The existence of stirrups significantly affected the behaviour of control deep beams. Presence of stirrups in corroded deep beams had no significant effect on their behaviour.
- Repair using FRP U-wraps was not effective in preventing the shear failure of the corroded deep beams.
- A strut and tie model was proposed to predict the ultimate strength of shear-critical reinforced concrete deep beams with corroded longitudinal reinforcement. The predicted results from the model were in reasonable correlation with the experimental results.
- The analytical model predicts that the failure mode of shear critical RC deep beams with corroded longitudinal reinforcement would change from splitting of compression strut to yielding of longitudinal reinforcement at higher concrete strengths and corrosion levels.

Acknowledgements

The authors would like to acknowledge the financial support in the form of graduate scholarship to the first author received from University of Engineering and Technology Lahore, Pakistan. The financial support received from the Natural Sciences and Engineering Research Council (NSERC) is also acknowledged. The donation of the concrete from Hogg Ready Mix is appreciated. Special thanks go to Dr. Ahmad El-Sayed for his contribution during the initial stages of this work. The help in laboratory work provided by the University of Waterloo technicians and the other members of the rehabilitation research group at the University of Waterloo is greatly appreciated.

References

[1] Kani GNJ. The riddle of shear failure and its solution. ACI J Proc 1964;61(4):441–68.
[2] Zararis PD, Papadakis GC. Diagonal shear failure and size effect in RC beams without web reinforcement. J Struct Eng, ASCE 2001;127(7):733–42.
[3] Aguilar G, Matamoros AB, Parra-Montesinos GJ, Ramirez JA, Wight JK. Experimental evaluation of design procedures for shear strength of deep reinforced concrete beams. ACI Struct J 2002;99(4):539–48.
[4] Al-Hammoud R, Soudki KA, Topper TH. Bond analysis of corroded reinforced concrete beams under monotonic and fatigue loads. Cem Concr Compos 2010;32(3):194–203.
[5] Chung L, Najm H, Balaguru P. Flexural behavior of concrete slabs with corroded bars. Cem Concr Compos 2008;30(10):184–93.
[6] Chung L, Kim J-HJ, Yi S-T. Bond strength prediction for reinforced concrete members with highly corroded bars. Cem Concr Compos 2008;30(7):603–11.
[7] Azad AK, Ahmad S, Azher SA. Residual strength of corrosion damaged reinforced concrete beams. ACI Mater J 2007;104(1):40–7.
[8] Bhargava K, Ghosh AK, Mori Y, Ramanujam S. Models for corrosion-induced bond strength degradation in reinforced concrete. ACI Struct J 2007;104(6):594–603.
[9] Wang X, Liu X. Bond strength modeling for corroded reinforcements. Constr Build Mater 2003;20:177–86.
[10] Higgins C, Farrow WC. Tests of reinforced concrete beams with corrosion-damaged stirrups. ACI Struct J 2006;103(1):133–41.
[11] Suffern C, El-Sayed A, Soudki K. Shear strength of disturbed regions with corrosion stirrups in reinforced concrete beams. Can J Civil Eng, CJCE 2010;37:1045–56.
[12] Xu S, Niu D. The shear behaviour of corroded reinforced concrete beam. In: International conference on advances in concrete and structures; 2003.
[13] El Maaddawy TA, Soudki KA. Effectiveness of impressed current technique to simulate corrosion of steel reinforcement in concrete. J Mater Civ Eng, ASCE 2003;15(3):41–7.
[14] ASTM G1. Standard practice for preparing, cleaning and evaluating test specimens. West Conshohocken (PA): ASTM International; 1990.
[15] Al-Hammoud R, Soudki K, Topper T. Fatigue flexural behaviour of corroded reinforced concrete beams repaired with CFRP sheets. J Compos Constr, ASCE 2011;15(1):42–51.
[16] El Maaddawy T, Soudki KA, Topper T. Performance evaluation of CFRP-repaired beams under corrosive environmental conditions. ACI Struct J 2007;104(1):3–11.
[17] CAN/CSA-A23.3-04. Design of concrete structures. Canadian Standard Association, Rexdale, Ontario, Canada; 2004. 240p.
[18] Adebar P, Zhou Z. Bearing strength of compressive struts confined by plain concrete. ACI Struct J 1993;90(5):534–41.